

Mass Spectrometry and Photoelectron Spectroscopy of *o*-, *m*-, and *p*-Terphenyl Cluster Anions: The Effect of Molecular Shape on Molecular Assembly and Ion Core Character

Masaaki Mitsui,[†] Naoto Ando,[†] and Atsushi Nakajima^{*,†,‡}

Department of Chemistry, Faculty of Science and Technology, Keio University, 3-14-1 Hiyoshi, Kohoku-ku, Yokohama 223-8522, Japan, and CREST, Japan Science and Technology Agency (JST), c/o Department of Chemistry, Keio University, Yokohama 223-8522, Japan

Received: February 8, 2008; Revised Manuscript Received: March 7, 2008

Mass spectrometry and photoelectron spectroscopy of *o*-, *m*-, and *p*-terphenyl cluster anions, (*o*-TP)_{*n*}⁻ (*n* = 2–100), (*m*-TP)_{*n*}⁻ (*n* = 2–100), and (*p*-TP)_{*n*}⁻ (*n* = 1–100), respectively, are conducted to investigate the effect of molecular shape on the molecular aggregation form and the resultant ion core character of the clusters. For (*o*-TP)_{*n*}⁻ and (*m*-TP)_{*n*}⁻, neither magic numbers nor discernible isomers are observed throughout the size range. Furthermore, their vertical detachment energies (VDEs) increase up to large *n* and depend linearly on *n*^{-1/3}, implying that they possess a three-dimensional (3D), highly reorganized structure encompassing a monomeric anion core. For (*p*-TP)_{*n*}⁻, in contrast, prominent magic numbers of *n* = 5, 7, 10, 12, and 14 are observed, and the VDEs show pronounced irregular shifts below *n* = 10, while they remain constant above *n* = 14 (isomer A). These results can be rationalized with two-dimensional (2D) orderings of *p*-TP molecules and different types of 2D shell closure at *n* = 7 and 14, the monomeric and multimeric anion core, respectively. Above *n* = 16, the new feature (isomer B) starts to appear at the higher binding side of isomer A, and it becomes dominant with *n*, while isomer A gradually disappears for larger sizes. In contrast to isomer A, the VDEs of isomer B continuously increase with the cluster size. This characteristic size evolution suggests that the transition to modified 2D aggregation forms from 2D ones occurs at around *n* = 20.

1. Introduction

π -Conjugated oligomers have been studied intensively from both fundamental and practical viewpoints for a long while. Due to their well-defined molecular structure and their ability to crystallize, they can serve as model compounds for the respective polymers and offer advantages over the polymers with regard to applications in new generations of (opto)electronic devices.¹ Since a profound knowledge of the electronic structure is indispensable for the device application, the electronic structure of thin solid films,^{2–4} single crystals,^{5–9} nanoparticles,^{10,11} and small clusters^{12–16} of π -conjugated oligomers has been investigated particularly in recent years. However, the influence of the intermolecular interaction/packing on the electronic structure has not been fully resolved.

Thus far, the occupied electronic levels, for example, the highest-occupied molecular orbital (HOMO), have been investigated to the last detail using various methods, such as photoemission yield spectroscopy and ultraviolet photoelectron spectroscopy (UPS). In particular, detailed UPS data are increasingly available from submonolayer to \sim 10 nm films.^{17–20} As reported recently, for instance, an angle-resolved UPS study of the well-ordered and well-oriented crystal film of *para*-hexaphenyl (*p*-HP) has demonstrated that there is a large intermolecular band dispersion of the occupied electronic levels in a direction perpendicular to the long molecular axis of the *p*-HP molecules, whereas it is absent in the direction parallel to the molecules.²⁰

In contrast, little experimental information is available about the unoccupied electronic levels, such as the lowest unoccupied molecular orbital (LUMO), in π -conjugated oligomer aggregates because their direct observation has been experimentally more difficult than that of the occupied levels. Recently, inverse photoemission spectroscopy (IPES) for thin films of various π -conjugated oligomers was performed to directly observe their unoccupied electronic levels, and the energetics of the LUMO, that is, polarization energy P_- for anions (the electrons) or solid-state electron affinity (A_s), have been evaluated.^{2–4} However, it seems that the typical energy resolution of IPES (400–500 meV) is still not enough to determine the precise values of A_s and P_- and to obtain the detailed experimental information about electron–phonon coupling as well as electron delocalization.

Molecular cluster ions of π -conjugated oligomers may serve as a cluster analogue of the bulk crystal, providing a well-defined microscopic description of charge localization and transport phenomena in organic crystals. It is possible to directly explore the electronic properties of a single excess charge doped with a finite-size molecular system under conditions that are completely free of chemical and physical impurities. In recent years, we have exploited anion photoelectron (PE) spectroscopy to follow the size-dependent energetics of the LUMO in clusters of π -conjugated oligomers including oligoacenes,^{21–25} oligophenyl,²⁶ and oligothiophene.²⁷ Indeed, the energetic changes of the LUMO going from an isolated molecule to the bulk can be clearly traced as a function of cluster size (*n*), offering a new avenue for estimating A_s .^{4,21–23} Furthermore, anion PE spectroscopy can provide direct information on the electron–vibrational coupling and, in some cases, electron delocalization (or charge resonance) effects at a specific molecular number and intermolecular geometry.^{13,14,28}

* To whom correspondence should be addressed. Fax: +81-45-566-1697. E-mail: nakajima@chem.keio.ac.jp.

[†] Faculty of Science and Technology.

[‡] JST-CREST.

As model compounds, we have herein chosen three-ring oligophenyl compounds, that is, *ortho*-terphenyl (*o*-TP), *meta*-terphenyl (*m*-TP), and *para*-terphenyl (*p*-TP), that are positional isomers having the same internal degrees of freedom. Thus, it will be helpful to compare the size evolution of electronic structure among these cluster anions in order to shed light upon the effect of molecular shape on the molecular aggregation form and the resultant ion core character of the cluster. In this Article, we will present results of mass spectrometry and anion PE spectroscopy of *o*-, *m*-, and *p*-TP cluster anions, $(o\text{-TP})_n^-$ ($n = 2\text{--}100$), $(m\text{-TP})_n^-$ ($n = 2\text{--}100$), and $(p\text{-TP})_n^-$ ($n = 1\text{--}100$), respectively. The comparison of the results obtained here highlights a singular behavior of $(p\text{-TP})_n^-$ going from the isolated molecule ($n = 1$) to the clusters ($n = 2\text{--}100$), which can be attributed to an inherent parallelism of highly anisotropic *p*-TP molecules, maximizing the intermolecular $\pi\text{--}\pi$ interaction cooperatively.

2. Experimental Section

Details of the experiment have been described previously.^{21,29–31} Briefly, the sample vapors of *p*-TP [melting point (mp): 213 °C], *m*-TP (mp 87 °C), or *o*-TP (mp 56 °C) were entrained in helium carrier gas at a stagnation pressure of 10–70 atm and underwent a supersonic expansion using a pulsed Even–Lavie valve.³² Cluster anions were produced by attachment of slow secondary electrons generated by a high-energy electron impact ionization method (~ 300 eV, ~ 10 mA) in the condensation zone in an expanding jet. The anions in the beam were coaxially extracted by applying a pulsed electric field ($-1.5 \sim -4.2$ kV) and were detected with a linear time-of-flight spectrometer having a mass resolution of $M/\Delta M \approx 150$. The target anions were selected and decelerated before photodetachment, which was initiated by 532 nm (2.331 eV) photons from a Nd³⁺:YAG laser. Each spectrum represents accumulation of 2000–20000 laser shots. In order to prevent Doppler broadening caused by the velocity of the ion beam, the smaller parent anions (mass number $< \sim 4000$) were impulsively decelerated down to several hundred eV prior to photodetachment. The resultant energy resolution was about 50 meV full width at half-maximum (fwhm) at 1 eV of electron kinetic energy. The PE spectrometer was calibrated with the $^1S_0 \rightarrow ^2S_{1/2}$ and $^1S_0 \rightarrow ^2D_{5/2}$ transitions of the gold atomic anion.

3. Results and Discussion

3.1. Mass Spectra for $(o\text{-TP})_n^-$, $(m\text{-TP})_n^-$, and $(p\text{-TP})_n^-$. Figure 1 displays mass spectra for $(o\text{-TP})_n^-$, $(m\text{-TP})_n^-$, and $(p\text{-TP})_n^-$ measured at stagnation pressure of ~ 30 atm. For $(o\text{-TP})_n^-$ and $(m\text{-TP})_n^-$, the monomer anion ($n = 1$) was not detected because of its negative or nearly zero gas-phase electron affinity (A_g),³³ and the smallest cluster anion detected was the dimer anion ($n = 2$). A smooth mass distribution with no intensity anomaly was always observed in both mass spectra under several sets of experiments. On the other hand, the mass spectrum of $(p\text{-TP})_n^-$, starting at $n = 1$, displays pronounced intensity anomalies at $n = 5$ and 7 as well as predominant formation of the even-numbered clusters of $n = 10, 12,$ and 14 (and also slightly at $n = 16, 18,$ and 19). It is noteworthy that the same magic numbers are also observed for cluster anions of *p*-quaterphenyl (*p*-QP), in which four phenyl rings are linked together in the *para*-position, though they are not observed for biphenyl (BP) cluster anions.³⁴ This fact implies that either an anisotropy of molecular shape or the number of aromatic rings serves as an important factor in the emergence of these magic numbers. Intensity anomalies in the mass distribution are often

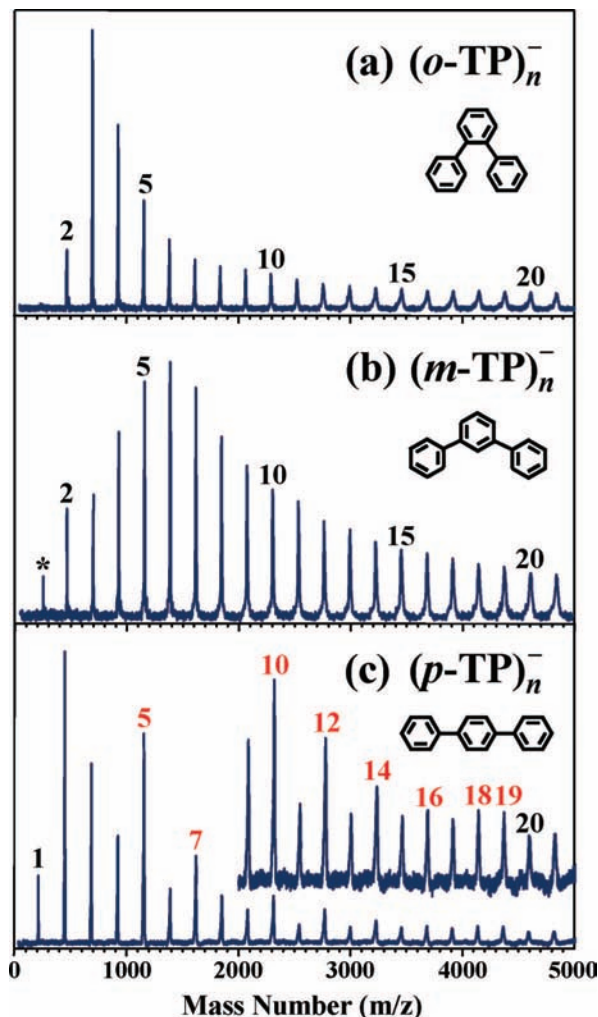


Figure 1. Mass spectra of (a) $(o\text{-TP})_n^-$, (b) $(m\text{-TP})_n^-$, and (c) $(p\text{-TP})_n^-$ recorded at a stagnation pressure of ~ 30 atm. In (b), “*” denotes a monohydrated *m*-TP anion. For only $(p\text{-TP})_n^-$, a reproducible magic number has arisen, labeled by red numbers (5, 7, 10, 12, 14, 16, 18, and 19).

attributable to geometrical shell closing of cluster ions^{14,23,35} or the appearance of a new electronic state,^{22,36,37} a proposition which will be discussed later. Above $n = 20$, this even–odd alternation disappears, and only a smooth intensity falloff is observed, like the case of $(o\text{-TP})_n^-$ or $(m\text{-TP})_n^-$.

3.2. PE Spectra for $(o\text{-TP})_n^-$, $(m\text{-TP})_n^-$, and $(p\text{-TP})_n^-$. Figure 2 shows the PE spectra for $(o\text{-TP})_n^-$ ($n = 2\text{--}100$), $(m\text{-TP})_n^-$ ($n = 2\text{--}100$), and $(p\text{-TP})_n^-$ ($n = 1\text{--}100$) measured at a photodetachment wavelength of 532 nm. The PE spectra for monomer anions ($n = 1$) of *o*-TP and *m*-TP could not be measured because of their nearly zero (or negative) electron affinities.³³ For $(o\text{-TP})_n^-$ and $(m\text{-TP})_n^-$, a structureless, single asymmetric band is monotonically shifted toward a binding energy as the cluster size increases, where no irregular peak shift is observed up to $n = 100$. Nevertheless, the internal degrees of freedom are identical between *o*-TP and *m*-TP, and yet, the PE spectra of $(o\text{-TP})_n^-$ is somewhat broader than those of $(m\text{-TP})_n^-$. This difference suggests that the amount of intermolecular rearrangement incurred in the geometrical change from the anion to the neutral is much larger in $(o\text{-TP})_n^-$ than that in $(m\text{-TP})_n^-$ and that there may be a large number of isoenergetic isomers in $(o\text{-TP})_n^-$. In fact, a remarkable broadening of the PE spectra was observed for $(o\text{-TP})_n^-$ ($n = 20\text{--}60$)

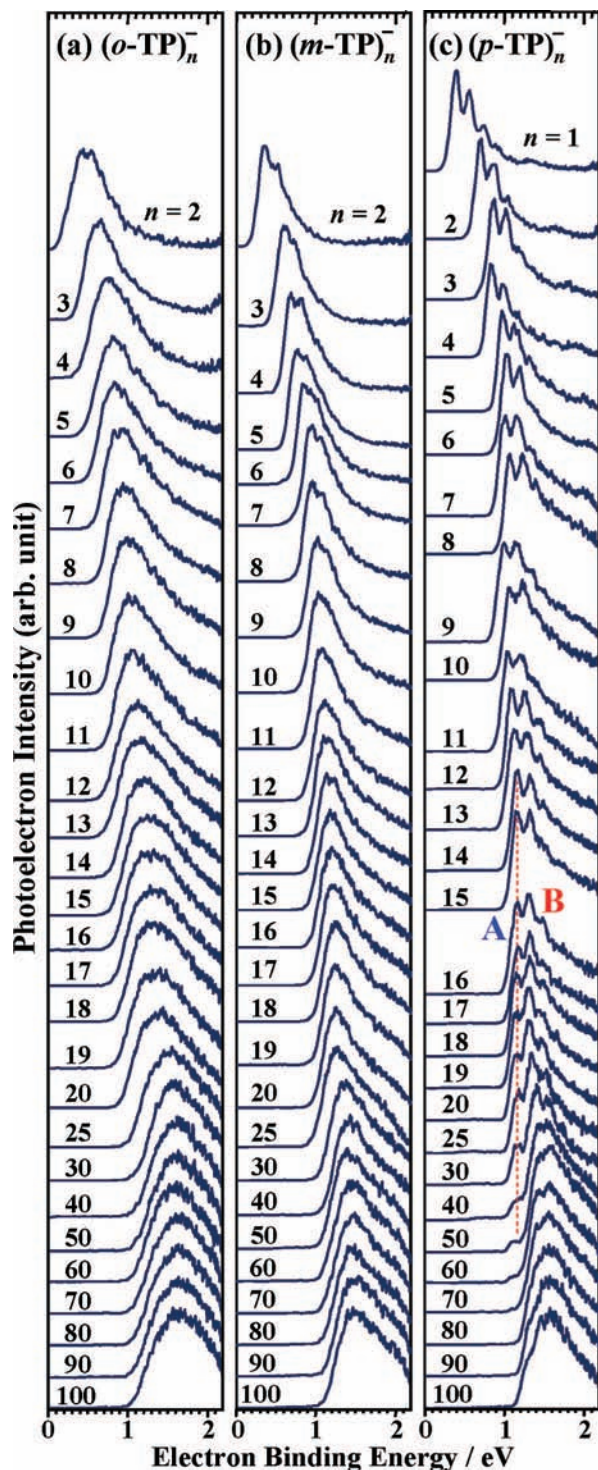


Figure 2. PE spectra for (a) $(o\text{-TP})_n^-$ ($n = 2\text{--}100$), (b) $(m\text{-TP})_n^-$ ($n = 2\text{--}100$), and (c) $(p\text{-TP})_n^-$ ($n = 1\text{--}100$) measured at 532 nm (2.331 eV).

under low He stagnation pressure conditions (<10 atm.), implying the presence of many isoenergetic isomers.

For $p\text{-TP}$, the A_g value can be determined to be 0.39 ± 0.01 eV from the electron binding energy of the first dominant peak in the PE spectrum of $n = 1$.³³ The partially resolved vibrational feature is also observed with an energy spacing of approximately 0.16 eV (ca. 1290 cm^{-1}),³⁸ which has been assigned to the interring C–C stretching mode ($\nu_{\text{C-C}}$) of neutral $p\text{-TP}$.³³ This vibrational structure is also clearly identified across the spectra from $n = 2$ to ~ 30 , signifying that the intermolecular modes

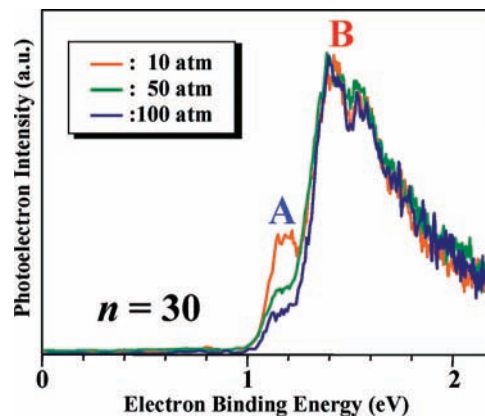


Figure 3. PE spectra of $(p\text{-TP})_{30}^-$ measured at different He stagnation pressures. As the stagnation pressure was increased, the intensity of band A decreased.

are hardly excited in the photodetachment process even at large cluster sizes. This spectral feature shows that the overall structural motif of $(p\text{-TP})_n^-$ must be closely similar to that of the corresponding neutral clusters.

The vertical detachment energy (VDE) of $(p\text{-TP})_n^-$ exhibits a peculiar size dependence. From $n = 1$ to 3, the VDE of the lowest origin-containing peak ($\nu_{\text{C-C}} = 0$) of the band is sharply shifted toward a higher binding energy with increasing cluster size. From $n = 3$ to 11, however, the VDE does not show a monotonic size dependence; it is shifted to lower binding energy at $n = 4, 7,$ and 9 (also slightly at $n = 11$), as can be seen in Figure 2c. Above $n = 12$, the VDE slightly increases up to $n = 14$ and then remains constant at 1.17 eV at $n \geq 14$. We hereafter designate this band as “A”.

Furthermore, a new feature labeled as “B”, which almost overlaps with the second vibrational peak ($\nu_{\text{C-C}} = 1$) of band A, appears around $n = 16$, and band B becomes more dominant with cluster size, while band A gradually disappears. In addition, it is importantly noted that the VDE of band B gradually increases with the cluster size, in contrast to no VDE shift of band A in $n = 14\text{--}50$.

These two bands can be attributed to the coexistence of two isomers. In order to reveal the coexistence, the change in the PE spectra was measured by varying the source pressure. Figure 3 shows the PE spectra of $n = 30$ obtained at different stagnation pressures; the relative intensity between bands A and B are changed, and the intensity of band A tends to decrease as the stagnation pressure increases. A similar dependence of the relative intensity between bands A and B was observed commonly at $n > 20$. These results suggest that the most stable anionic form is switched from “isomer A” (band A) to “isomer B” (band B) beyond $n \approx 16$.

In order to show the presence of these isomers clearly, the PE spectra of $(p\text{-TP})_n^-$ for $n = 14\text{--}30$ were deconvoluted into two components of isomers A and B, with the results shown in Figure 4. For $n = 14$, a set of four Gaussian functions with an equal energy spacing of the $\nu_{\text{C-C}}$ mode (ca. 0.16 eV) reproduces the PE spectrum (i.e., the profile of isomer A). However, the PE spectra of $n = 16\text{--}30$ cannot be reproduced using only the single set of Gaussian functions, exhibiting the mixture of the other component. Here, the higher-energy component (band B) is obtained by the subtraction of the contribution of band A from the whole envelope at each n . As a result, the anomalous profiles can be reproduced by the overlapping of two sets of Gaussian functions. Although we cannot rule out the possibility that the spectra for $n \leq 15$ also contain a high-energy band

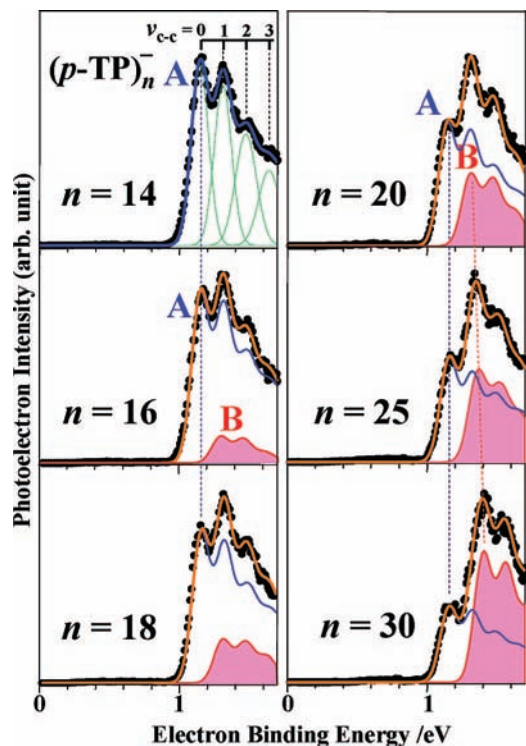


Figure 4. Analysis of PE spectra for $(p\text{-TP})_n^-$ with $n = 14, 16, 18, 20, 25,$ and 30 using one (or two) set(s) of three/four Gaussian functions, which present an origin transition as well as vibrational progression of the ν_{c-c} mode. The experimental PE spectra are shown by filled circles. Deconvolution of the experimental data is shown by blue (band A) and red (band B) lines.

TABLE 1: Vertical Detachment Energies (VDEs) of $(p\text{-TP})_n^-$ ($n = 1\text{--}100$) Cluster Anions in eV

VDE		VDE		
n	isomer A	n	isomer A	isomer B
1	0.39(1) ^a	20	1.17(3)	1.33(2)
2	0.69(1)	21	1.17(3)	1.35(2)
3	0.85(1)	22	1.17(3)	1.36(2)
4	0.84(1)	23	1.17(3)	1.36(2)
5	1.00(1)	24	1.17(3)	1.35(2)
6	1.05(1)	25	1.17(3)	1.36(2)
7	1.04(1)	26	1.17(3)	1.38(2)
8	1.09(1)	27	1.17(3)	1.40(2)
9	1.05(1)	28	1.17(3)	1.41(2)
10	1.11(1)	29	1.17(3)	1.40(2)
11	1.11(1)	30	1.17(3)	1.42(3)
12	1.13(2)	35	1.17(4)	1.44(4)
13	1.15(2)	40	1.17(4)	1.45(4)
14	1.17(2)	50	1.17(4)	1.49(4)
15	1.17(2)	60		1.50(4)
16	1.17(2)	70		1.52(4)
17	1.17(2)	80		1.53(4)
18	1.17(2)	90		1.54(4)
19	1.17(3)	100		1.54(4)
				1.32(2)
				1.33(2)
				1.33(2)
				1.34(2)

^aFrom ref 33. Numbers in parentheses indicate uncertainties in VDE values; 0.39(1) represents 0.39 ± 0.01 .

(isomer B), it is obviously a minor component. Note that the overall spectral feature does not change markedly below $n \approx 20$ under various ion source conditions. The VDEs of $n = 1\text{--}100$ (isomers A and B) obtained are summarized in Table 1.

3.3. Presumed Aggregation Forms and Ion Core Characters of $(p\text{-TP})_n^-$ ($n = 2\text{--}20$). As shown in Figure 5, the VDE values of $n = 1\text{--}20$ (VDEs of isomer B in $n \geq 16$ not shown) obtained by the deconvolution of the PE spectra are

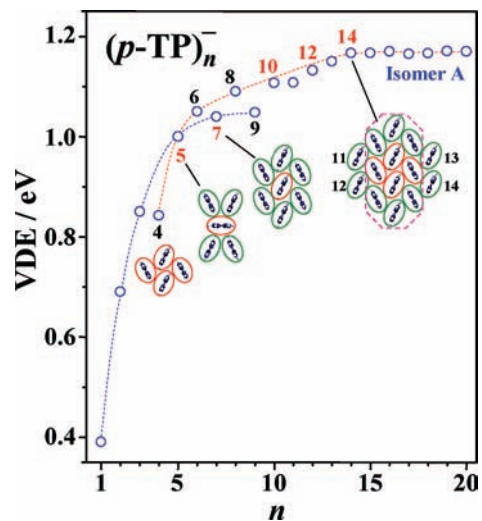


Figure 5. Plots of VDEs of $(p\text{-TP})_n^-$ as a function of cluster size, n , for $n = 1\text{--}20$. Red and green dashed lines linking each data point of $n = 1\text{--}3, 5, 7,$ and 9 and $n = 4, 6, 8, 10, 12,$ and ≥ 14 , respectively, are guides for the eye. The VDE of isomer A becomes constant above $n = 14$. Proposed geometrically closed 2D structures for $n = 4, 5, 7,$ and 14 , where the long molecular axes are assumed to be parallel to one another, are also shown. Red and blue ellipsoids represent the ion core and the first 2D shell, respectively. The 10-mer unit surrounded by a pink dotted line may correspond to a partial shell closing in the 2D structure.

plotted against cluster size n . Below $n = 10$, there is the striking difference in the VDE energetics between the even-numbered clusters of $n = 4, 6, 8,$ and 10 and the odd-numbered clusters of $n = 3, 5, 7,$ and 9 . In Figure 5, two different dashed lines join each of the VDE data for clarity. In general, the VDE [and also adiabatic detachment energy (ADE)] values of the cluster anions having an identical ion core increase monotonically with increasing cluster size,^{39,40} owing to an additional charge stabilization by the addition of a neutral molecule. Therefore, it is likely that the *p*-TP cluster anions ($n \leq 10$), that is, isomer A, possess distinct anion cores at the even- and odd-numbered sizes.

It is worthy of note that although the VDE of $n = 7$ is smaller than those of $n = 6$ and 8 , the $n = 7$ cluster is more abundantly produced than the even-numbered neighbors (see Figure 1c). This result would be ascribed to a consequence of a unique geometry, for example, a geometrically closed-shell structure. Since *p*-TP has a highly anisotropic molecular shape (its long molecular axis is ca. 14 Å), a two-dimensional (2D) aggregation tends to occur preferentially through the anisotropic intermolecular $\pi\text{-}\pi$ interaction.^{10,41,42} Very recently, for the (tetracene)_n⁻ clusters with $n = 2\text{--}50$, we have reported that tetracene molecules, whose molecular length (ca. 12 Å) is comparable to that of *p*-TP, aggregate themselves into the 2D herringbone-type arrangement.²³ Thus, it can be presumed that *p*-TP molecules also show a 2D herringbone-type ordering in the cluster, where all of the long molecular axes are parallel. As schematically illustrated in Figure 5, we propose a 2D shell closure at $n = 7$, where a central monomeric ion is two-dimensionally enclosed by the other six molecules. After the first shell closure, stabilization of the central ion would become much less efficient due to the charge screening by the first coordination shell as well as the longer ion-molecular distances. Indeed, the rate of increase in the VDE from $n = 7$ to 9 is very small (only 0.01 eV) compared to that of $n = 5$ to 7 (0.04 eV). As a result, it is probable that the 2D structure with the

monomeric ion core becomes no longer for the preferred stable form in $n \geq 10$.

As seen in Figure 1c, the $n = 5$ cluster is the most intense magic number in the mass spectrum. It might possess a less geometrically closed 2D structure (e.g., a half-filled 2D shell) with the loss of two molecules from the 2D shell-closed unit of $n = 7$. However, it is noted that the $n = 5$ cluster is observed as a common magic number in $(p\text{-TP})_n^-$, while the intensity anomaly at $n = 7$ is not observed for the mass spectrum of $(\text{tetracene})_n^-$.²³ Moreover, the prominent formation at $n = 5$ has also been observed for the related aromatic cluster anions, such as $(\text{anthracene})_n^-$ (ref 13) and $(p\text{-QP})_n^-$ (ref 34). Hence, it appears that there is some unique geometric and/or electronic stability in the pentamer anions of these π -conjugated oligomers. One plausible geometry for the pentamer anion is the 2D structure where the hydrogen atoms of two neutral molecules attach on each side of the π rings of the molecular anion with tilted T-shaped geometries, such as shown in Figure 5. This structure can be recognized as a virtual 2D shell-closed structure for the monomeric anion core because the excess charge on the π rings of the ion is almost completely surrounded by the neutral molecules through π -hydrogen bonding interactions. Indeed, the rate of increase in the VDE from $n = 5$ to 7 (0.04 eV) is much smaller than that from $n = 3$ to 5 (0.15 eV), indicating that the effective shielding of the excess charge is almost completed at $n = 5$. By the addition of two molecules, the model structure proposed for $n = 5$ can probably evolve into the 2D shell-closed structure of $n = 7$ with relatively small orientational rearrangements of surrounding neutrals. For these structures, however, it is deemed that some support from theoretical models is imperative in future work.

As mentioned above, however, the predominant formation of $n = 7$ is not observed for $(\text{anthracene})_n^-$ and $(\text{tetracene})_n^-$ because the anion state with a three-dimensional (3D) monomeric ion core structure (referred to as "isomer I" in refs 21, 23, and 24) is produced preferentially at $n = 7$. Note that the molecular lengths of anthracene and tetracene (ca. 9 and 12 Å, respectively) are shorter than that of $p\text{-TP}$ (ca. 14 Å). In addition, the magic number at $n = 7$ is not observed for those of BP (molecular length: ca. 9 Å), whereas it is observed for the cluster anions of $p\text{-QP}$ (ca. 18 Å).³⁴ Therefore, it is evident that the structural anisotropy of the cluster constituents dominates the formation of a 2D isomeric form at $n = 7$ (and also neighboring sizes). Namely, longer (or anisotropic) molecular frameworks of the constituents prefer 2D molecular assemblies in small cluster sizes ($n < 10$). Considering all of the results described, the threshold for appearance of a 2D structure at $n = 7$ appears to lie within the molecular length of 12–14 Å.

On the other hand, the VDEs of the even-numbered clusters in $n = 6$ –14, which are larger than those of the odd-numbered clusters ($n = 7$ and 9), show a smooth size dependence. The size evolution implies that they have an identical ion core within the even-numbered clusters. It is emphasized that the irregular VDE shift begins to appear at $n = 4$, whose VDE cannot be linked to that of $n = 3$, as seen in Figure 5. This break suggests that the ion core switching occurs from $n = 3$ to 4 and that the ion core of the tetramer anion is not so much monomeric as multimeric in nature. For the $(p\text{-TP})_4^-$ cluster, our preliminary calculations using density functional theory (DFT) at the B3LYP/6-31G level of theory yield a cyclic C_2 geometry (similar to a proposed structure for $n = 4$ shown in Figure 5) as a minimum-energy structure, where the excess electron is delocalized over all four constituents of the cluster. At present, however, it is not clear that the DFT calculations can properly

assess charge resonance interactions in homogeneous π -conjugated molecular cluster ions,¹⁶ and thus, the ion core character in $(p\text{-TP})_4^-$ requires further theoretical verifications. In any case, it is highly probable that the even-numbered clusters in $n = 4$ –14 have an identical multimeric (presumably tetrameric) ion core that yields a larger VDE than the (hypothetical) monomeric core anion cluster. Since the VDE corresponds to the energy difference between the anion and neutral at the equilibrium geometry of the anion, the magnitude of VDE includes the contribution of reorganization energy (RE) as well as ADE (i.e., $\text{VDE} = \text{ADE} + \text{RE}$). In $n = 2$ –14, no significant difference was observed in the PE envelopes between the even- and odd-numbered clusters, so that the contribution of RE to the magnitude of VDE should be comparable between them. Thus, the larger VDEs of the even-numbered clusters ($n = 6, 8,$ and 10) than those of $n = 7$ and 9 may simply come from the increased ADE through charge resonance interaction within a multimeric ion core moiety. On the contrary, however, it is currently difficult to explain why the monomeric ion core is exclusively produced at $n = 9$; it can surpass the "hypothetical" multimeric ion core isomer in the relative stability. For $n = 9$, no geometrical stabilization effect is expected because it is not a magic number in the mass spectrum. Conceivably, the $(p\text{-TP})_9^-$ cluster has intrinsically no stable 2D structure with a multimeric anion core, and the stable 2D geometry of $n = 9$ may necessarily impose the monomeric anion character upon itself. Interestingly, note that, in the $(\text{anthracene})_9^-$ and $(\text{tetracene})_9^-$ clusters, the monomeric-anion core state is provided by a 3D aggregation form (referred to as "isomer I" in refs 23 and 24), like the case of their $n = 7$ clusters. In a qualitative sense, this difference thus signifies that more $p\text{-TP}$ molecules preferably aggregate into a 2D form than anthracene and tetracene molecules.

Intriguingly, the VDEs of $(p\text{-TP})_n^-$ remain constant above $n = 14$ (isomer A). The incremental rate in VDE often becomes abruptly smaller after the completion of the first solvation shell^{24,39,40} because of the longer ion–molecular distances and the screening effect of the central excess charge. Furthermore, since the magnitude of VDE is governed not only by the energetics but also by structural factors (i.e., RE), the constant VDEs signify that the amount of structural relaxation incurred in the geometric change from the anion to the neutral no longer depends on the cluster size above $n = 14$. Hence, it is concluded that the constant VDEs above $n = 14$ indicate the establishment of a stable (or rigid) shell-closed 2D unit at the $n = 14$ cluster.

As illustrated in Figure 5, a presumed structure for the $n = 14$ cluster can constitute the first 2D shell closure for the tetramer core, where 10 molecules completely and densely fill the first 2D shell for the central four molecules. In this structure, it is expected that the charge screening effect is rather efficient, leading to the invariable nature of VDE for $n \geq 14$.²³ Additionally, the predominant formation of $n = 10, 12,$ and 14 can be rationalized by the 2D aggregation form of the type shown in Figure 5. In the 14-mer shown in Figure 5, for example, the 2D shell around a 10-mer unit (surrounded by a pink dotted line) can be filled by molecules 11–14, and the shell/subshell closings occur at 10, 12, and 14, which indeed appear as local maxima in the mass spectrum. For $n \geq 15$, the slight intensity anomaly at $n = 16, 18,$ and 19 implies that additional molecules may further enclose two-dimensionally the 14-mer unit in a stepwise fashion, like the case of $(\text{tetracene})_n^-$.²³ However, no intensity anomaly is discernible beyond $n = 20$, which is due to the gradual population reduction of the 2D clusters (i.e., isomer A) above $n \approx 16$ (see Figure 2c or 4).

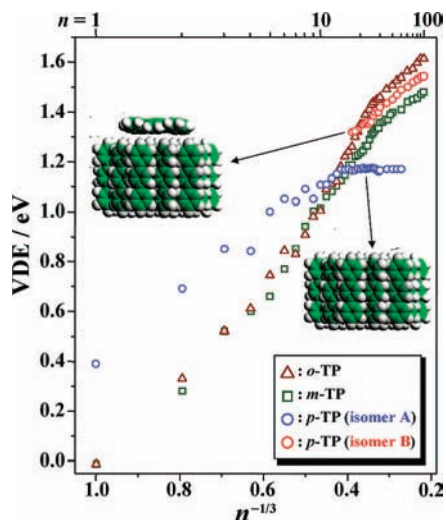


Figure 6. VDE plots for $(o\text{-TP})_n^-$, $(m\text{-TP})_n^-$, and $(p\text{-TP})_n^-$ (isomers A and B) against $n^{-1/3}$ for $n = 1-100$. For $n = 1$, the values of the gas-phase electron affinity A_g are taken from ref 33. Schematic illustrations of 2D (isomer A) and modified 2D (isomer B) structures are also shown.

3.4. VDE Energetics for $(o\text{-TP})_n^-$, $(m\text{-TP})_n^-$, and $(p\text{-TP})_n^-$.

In Figure 6, the VDEs of $(o\text{-TP})_n^-$ ($n = 2-100$), $(m\text{-TP})_n^-$ ($n = 2-100$), and $(p\text{-TP})_n^-$ (isomers A and B in $n = 1-100$) are plotted as a function of $n^{-1/3}$. It is clear that the VDEs of $(o\text{-TP})_n^-$ and $(m\text{-TP})_n^-$ increase almost linearly with $n^{-1/3}$ and reach ~ 1.6 and 1.5 eV at $n^{-1/3} \approx 0.215$ ($n = 100$), respectively. Least-squares fits of the VDE data of $n = 30-100$ yield the extrapolated VDE [VDE(∞)] values of 1.93 eV for $(o\text{-TP})_n^-$ and 1.72 eV for $(m\text{-TP})_n^-$. Although no negative polarization energy P_- of solid oligophenyls has been reported as far as we know, the typical value of P_- for oligoacene crystals resides around 1 eV.^{43,44} Since A_s is given by $A_g + P_-$ (ref 4) and the values of A_g for *o*-TP and *m*-TP are ≈ 0 eV,³³ A_s for $(o\text{-TP})_n^-$ and $(m\text{-TP})_n^-$ can be estimated to be about 1 eV, which is 0.7–0.9 eV smaller than the VDE(∞) values obtained here. This discrepancy indicates that RE makes a considerable contribution to the VDE(∞) = $A_s + \text{RE} = A_g + P_- + \text{RE}$. Here, RE is the total between the structural rearrangement energy in the neutral state and that in the anion state. Namely, the RE values of $(o\text{-TP})_n^-$ and $(m\text{-TP})_n^-$ at $n = \infty$ can be roughly estimated to be ~ 0.9 and 0.7 eV, respectively. Note that the comparable RE values have been obtained for oligoacene cluster anion systems^{24,25} and may be attributed to relatively large quadrupole moments of π -conjugated oligomers. The results therefore indicate that large cluster anions of *o*-TP and *m*-TP are produced through electron attachment to preformed neutral clusters followed by significant intermolecular rearrangement of neutral molecules that encompass the monomer anion three-dimensionally. In other words, they possess a highly reorganized 3D structure with the monomer anion occupying the internalized position in the cluster. In this case, the VDE(∞) value can be much larger than the extrapolated ADE [ADE(∞)] value that corresponds to A_s . As seen in Figure 1a and b, in addition, the PE spectra for $(o\text{-TP})_n^-$ and $(m\text{-TP})_n^-$ display broad structureless envelopes, as is typically the case.

On the other hand, the VDEs of isomer A in $(p\text{-TP})_n^-$ converge to the constant value of 1.17 eV at $n = 14$, resulting from the establishment of a 2D shell-closed unit by 14 *p*-TP molecules, as described above. Compatibly, the relatively sharp PE profile of isomer A, exhibiting a vibrational progression of the $\nu_{\text{C-C}}$ mode (see Figure 2c), indicates that isomer A can be

confidently assigned to the anion formed from preformed neutral clusters without (or with much less) intermolecular geometrical relaxation (i.e., RE \approx 0). Thus, the constant VDE value of 1.17 eV may be regarded as an approximate ADE value of $n \geq 14$. It is noted that the establishment of such a “rigid” 2D shell-closed unit at the 14-mer has been also found for the cluster anions of anthracene²⁴ and tetracene²³ (where this type of 2D cluster anions were designated as “isomer II-1”).

The total (vertical) charge stabilization energy (ΔE_{tot}) for isomer A (i.e., a finite 2D *p*-TP monolayer) can be estimated to be -0.78 eV by summing the A_g value of a *p*-TP molecule (0.39 eV) and the constant $-VDE$ value (-1.17 eV). Due to the invariant nature of VDE for $n \geq 14$, the value of -0.78 eV may be recognized as an asymptotic ΔE_{tot} for an isolated infinite 2D monolayer of *p*-TP. In other words, it may correspond to a 2D polarization energy of the bulk. Importantly, if we assume that the polarization energy P_- of a *p*-TP crystal is 1 eV, only 14 *p*-TP molecules in a 2D herringbone-type layer can provide $\sim 80\%$ of that of the crystal. It is worth noting that the ΔE_{tot} value obtained for the 2D *p*-TP monolayer is slightly larger than that for the 2D monolayer of tetracene, that is, -0.74 eV, which has been determined from the results of PE spectroscopy for $(\text{tetracene})_n^-$ ($n = 1-100$).²³

As is well-known, an approximate relation of the polarization energy (P) indicates that P is proportional to $\alpha p^{4/3}$, where α is the average molecular polarizability and p is the molecular packing density.⁴ The value of α for *p*-TP (35.56×10^{-30} m³) is a little larger than that for tetracene (32.27×10^{-30} m³).⁴ Therefore, if we assume that p is the same between the *p*-TP and tetracene 2D monolayers, the value of P for the *p*-TP monolayer should be 1.10 times larger than that for the tetracene monolayer. However, the ratio of ΔE_{tot} between the *p*-TP and tetracene 2D monolayers is 1.05 ($= -0.78$ eV/ -0.74 eV), which is slightly smaller than the ratio of α between the *p*-TP and tetracene molecules (i.e., 1.10). In contrast to tetracene, it should be noted that a *p*-TP molecule has the degrees of freedom of intramolecular rotation by the angle around a single C–C bond linking each phenyl ring, and the conformation can be thus influenced through the molecular aggregation. In the gas phase, a *p*-TP molecule is twisted due to the steric repulsion between *ortho*-hydrogen atoms, whereas in the crystals, *p*-TP molecules seemingly prefer planar conformations due to the packing effect.⁴⁵ Thus, the difference mentioned above suggests a slightly smaller packing density of the *p*-TP monolayer cluster than that of the tetracene monolayer cluster, the origin of which may be due to nonplanar conformations of neutral *p*-TP molecules in $(p\text{-TP})_n^-$.

3.5. Switching of the Aggregation Form of $(p\text{-TP})_n^-$ ($n \geq 16$). Above $n = 16$ in $(p\text{-TP})_n^-$, isomer B starts to appear at ~ 0.2 eV to the higher electron binding side of isomer A and gradually becomes dominant under any source conditions (see Figures 2c and 4), showing that isomer B becomes more energetically stable than isomer A at larger cluster sizes. It is emphasized that such an isomer has not been observed for $(o\text{-TP})_n^-/(m\text{-TP})_n^-$ and for biphenyl cluster anions.³³ In contrast to the constant VDE of isomer A, the VDEs of isomer B continuously increase with the cluster size, and their size dependence is very similar to those of $(o\text{-TP})_n^-$ and $(m\text{-TP})_n^-$ as seen in Figure 6. At first glance, this similarity seemingly points out that isomer B corresponds to a highly reorganized 3D cluster anion with a monomeric ion core, like $(o\text{-TP})_n^-$ and $(m\text{-TP})_n^-$. However, the analysis of the PE spectra for $n = 16-30$ (see Figure 4) reveals that band B has a discernible vibrational structure of the $\nu_{\text{C-C}}$ mode, which is also observed

in band A. This feature indicates that the intermolecular modes are not highly excited in the photodetachment process; the intermolecular geometry between neutral molecules surrounding the ion core is not significantly rearranged with the photodetachment event. Thus, isomer B with $n = 16\text{--}30$ cannot be simply ascribed to highly reorganized 3D cluster anions such as those produced in $(o\text{-TP})_n^-$ and $(m\text{-TP})_n^-$.

For the small size region of $(p\text{-TP})_n^-$ ($n \leq 15$), the present results show that the 2D cluster anions are formed exclusively, implying their higher stability than the reorganized 3D aggregation forms. Therefore, although we can only conjecture the structures involved in isomer B, it is tempting to presume that additional neutral molecules are attached onto a plane of the 2D monolayer unit, as schematically illustrated in Figure 6. In this structure, the additional molecules after the first 2D shell closure at $n = 14$ can attach to positions more proximal to the ion core and stabilize it more efficiently than the 2D structural motif (i.e., isomer A with $n \geq 15$). As a result, it is probable that the VDEs (or ADEs) of isomer B can further increase with the cluster growth.

As reported recently, in $(\text{tetracene})_n^-$, an additional isomer with a constant VDE (referred to as "isomer II-2" in ref 23) emerges above $n = 60$ and is produced only at high source pressures. Since the constant VDE value shows a good agreement with the corresponding A_s value, this type of isomer has been assigned to the crystal-like anion state where two or more finite 2D herringbone layers are stacked.^{23–25} For $(p\text{-TP})_n^-$ (up to $n = 100$), in contrast, such a crystal-like multilayered isomer does not appear at all under any source conditions. This result suggests that the multilayered cluster anion (corresponding to isomer II-2) is energetically less stable than isomer B, which probably possesses the modified 2D forms, as mentioned above.

In the recent study on anthracene and its alkyl-substituted anthracene cluster anions,²⁴ we have found that there is an evident correlation in the formation of isomers II-1 (i.e., a 2D monolayer cluster) and II-2 (i.e., a double-layered or more multilayered cluster). That is, isomer II-1 can be a precursor form of isomer II-2. As mentioned in section 3.3, the 2D cluster anions (isomer A) tend to be more favorably produced in $(p\text{-TP})_n^-$ than in $(\text{tetracene})_n^-$ at small sizes ($n < 10$), ensuring the high stability of the 2D herringbone-type monolayer (isomer A). Furthermore, the crystal structure of $p\text{-TP}$ has stacked herringbone layers, the structural motif of which is commonly found in oligoacene crystals. Considering these facts, we can expect that the multilayered cluster anion (corresponding to the isomer II-2) should be also produced in large $(p\text{-TP})_n^-$ clusters. Therefore, no formation of the multilayered isomer in $(p\text{-TP})_n^-$ suggests that there are some crucial differences between $p\text{-oligophenyl}$ and oligoacene cluster anions.

In the oligoacene cluster anions, the 2D isomer (isomer II-1) usually coexists with the highly reorganized 3D one (referred to as "isomer I" in refs 21–25) at small sizes ($n < \sim 14$), but the relative stability of the latter gradually exceeds that of the former with increasing cluster size from $n = \sim 15$ to ~ 60 . In the much larger size region ($n > \sim 60$), however, the crystal-like multilayered form (isomer II-2) surpasses the reorganized isomer (isomer I) in the relative stability due to the additional charge stabilization (typically ~ 0.2 eV) provided by neutral molecules in the adjacent layer(s).^{23–25} In the case of $(p\text{-TP})_n^-$, in contrast, the present study shows that the 2D cluster (isomer A) is formed exclusively in the small size region ($n < 16$) and, in larger sizes, followed by the formation of the modified 2D structural motif (isomer B) that can provide an additional stabilization (≥ 0.15 eV; see Table 1) for the excess charge in

the 2D layer. Therefore, it is probable that the presence of isomer B can energetically prohibit the formation of the crystal-like multilayered form in the $(p\text{-TP})_n^-$ clusters. Additionally, note that the molecular structure and excess charge density/distribution around terminal ends along the long molecular axis are evidently different between $p\text{-oligophenyl}$ and oligoacene molecules, which could also influence the stability of multilayered molecular assemblies.

4. Conclusions

In this work, we have reported the mass spectrometry and PE spectroscopy of $o\text{-}$, $m\text{-}$, and $p\text{-TP}$ cluster anions ($n = 2\text{--}50$). The present study reveals the effect of molecular shape on molecular aggregation forms and the resultant ion core characters of the clusters. Striking differences were clearly identified between the results of $(o\text{-TP})_n^-/(m\text{-TP})_n^-$ and $(p\text{-TP})_n^-$. For $(o\text{-TP})_n^-$ and $(m\text{-TP})_n^-$, no magic number and no additional isomer are observed over the entire size range examined. In addition, the VDEs continuously increase over the range of $n = 2\text{--}50$, and almost all of them depend linearly on $n^{-1/3}$ because of the effects of electronic polarization and intermolecular reorganization of neutral molecules encompassing a monomeric anion core three-dimensionally. For $(p\text{-TP})_n^-$, in contrast, clear magic numbers at $n = 5, 7, 10, 12$, and 14 and the pronounced irregular shifts of the VDEs are observed below $n = 10$, while the VDEs remain constant above $n = 14$ (isomer A). These results can be explained well by 2D arrangements of $p\text{-TP}$ molecules and different types of 2D enclosures at $n = 7$ and 14, which probably have monomeric and tetrameric anion cores, respectively. Above $n = 16$, however, a new feature (isomer B) begins to appear at 0.2 eV on the higher binding side of isomer A, and it becomes dominant with n , while isomer A gradually disappears in larger sizes. The characteristic size evolution can be explained by the formation of crystal-like 2D aggregation forms with a transition toward modified 2D ones as the cluster grows in size.

Acknowledgment. This work is partly supported by Grant-in-Aids for Young Scientists (B), No. 14740332 and No. 17750016, and on Priority Area "Molecular Theory for Real Systems", No. 19029041. N. A. is grateful to JSPS Research Fellowships for Young Scientists.

References and Notes

- Witte, G.; Wöll, C. *J. Mater. Res.* **2004**, *19*, 1889.
- Hill, I. G.; Kahn, A.; Soos, Z. G.; Pascal, R. A., Jr. *Chem. Phys. Lett.* **2000**, *327*, 181.
- Amy, F.; Chan, C.; Kahn, A. *Org. Electron.* **2005**, *6*, 85.
- Seki, K.; Kanai, K. *Mol. Cryst. Liq. Cryst.* **2006**, *455*, 145, and references therein.
- Tsiper, E. V.; Soos, Z. G. *Phys. Rev. B* **2001**, *64*, 195124.
- Tsiper, E. V.; Soos, Z. G. *Phys. Rev. B* **2003**, *68*, 085301.
- Cornil, J.; Calbert, J. Ph.; Brédas, J. L. *J. Am. Chem. Soc.* **2001**, *123*, 1250.
- Deng, W.; Goddard, W. A., III. *J. Phys. Chem. B* **2004**, *108*, 8614.
- Cheng, Y. C.; Silbey, R. J.; da Silva Filho, D. A.; Calbert, J. P.; Cornil, J.; Brédas, J. L. *J. Chem. Phys.* **2003**, *118*, 3764.
- Blumstengel, S.; Meinardi, F.; Spearman, P.; Borghesi, A.; Tubino, R.; Chirico, G. *J. Chem. Phys.* **2002**, *117*, 4517.
- Oelkrug, D.; Egelhaaf, H.-J.; Gierschner, J.; Tompert, A. *Synth. Met.* **1996**, *76*, 249.
- Song, J. K.; Han, S. Y.; Chu, I.; Kim, J. H.; Kim, S. K.; Lyapunina, S. A.; Xu, S.; Nilles, J. M.; Bowen, K. H., Jr. *J. Chem. Phys.* **2002**, *116*, 4477.
- Song, J. K.; Lee, N. K.; Kim, S. K. *Angew. Chem., Int. Ed.* **2003**, *42*, 213.
- Song, J. K.; Lee, N. K.; Kim, J. H.; Han, S. Y.; Kim, S. K. *J. Chem. Phys.* **2003**, *119*, 3071.
- Hutchison, G. R.; Ratner, M. A.; Marks, T. J. *J. Am. Chem. Soc.* **2005**, *127*, 16866.

- (16) Bouvier, B.; Brenner, V.; Millié, P.; Soudan, J. *J. Phys. Chem. A* **2002**, *106*, 10326.
- (17) Sato, N.; Seki, K.; Inokuchi, H. *J. Chem. Soc., Faraday Trans. II* **1981**, *77*, 1621.
- (18) Salaneck, W. R.; Seki, K.; Kahn, A.; Pireaux, J.-J., Eds. *Conjugated Polymer and Molecular Interfaces*; Marcel Dekker: New York, 2001.
- (19) Koch, N.; Vollmer, A.; Salzmann, I.; Nickel, B.; Weiss, H.; Rabe, J. P. *Phys. Rev. Lett.* **2006**, *96*, 156803-1.
- (20) Koller, G.; Berkebile, S.; Oehzelt, M.; Puschnig, P.; Ambrosch-Draxl, C.; Netzer, F. P.; Ramsey, M. G. *Science* **2007**, *317*, 351.
- (21) Mitsui, M.; Kokubo, S.; Ando, N.; Matsumoto, Y.; Nakajima, A.; Kaya, K. *J. Chem. Phys.* **2004**, *121*, 7553.
- (22) Mitsui, M.; Nakajima, A. *Bull. Chem. Soc. Jpn.* **2007**, *80*, 1058.
- (23) Mitsui, M.; Ando, N.; Nakajima, A. *J. Phys. Chem. A* **2007**, *111*, 9644.
- (24) Ando, N.; Mitsui, M.; Nakajima, A. *J. Chem. Phys.* **2007**, *127*, 234305.
- (25) Ando, N.; Mitsui, M.; Nakajima, A. *J. Chem. Phys.* Submitted.
- (26) Mitsui, M.; Matsumoto, Y.; Ando, N.; Nakajima, A. *Chem. Lett.* **2005**, *34*, 1244.
- (27) Mitsui, M.; Matsumoto, Y.; Ando, N.; Nakajima, A. *Eur. Phys. J. D* **2005**, *34*, 169.
- (28) Ando, N.; Kokubo, S.; Mitsui, M.; Nakajima, A. *Chem. Phys. Lett.* **2004**, *389*, 279.
- (29) Nakajima, A.; Taguwa, T.; Hoshino, K.; Sugioka, T.; Naganuma, T.; Ono, F.; Watanabe, K.; Nakao, K.; Konishi, Y.; Kishi, R.; Kaya, K. *Chem. Phys. Lett.* **1993**, *214*, 22.
- (30) Mitsui, M.; Nakajima, A.; Kaya, K.; Even, U. *J. Chem. Phys.* **2001**, *115*, 5707.
- (31) Mitsui, M.; Nakajima, A.; Kaya, K. *J. Chem. Phys.* **2002**, *117*, 9740.
- (32) Even, U.; Jortner, J.; Noy, D.; Lavie, N.; Cossart-Magos, C. *J. Chem. Phys.* **2000**, *112*, 8068.
- (33) Nakamura, T.; Ando, N.; Matsumoto, Y.; Furuse, S.; Mitsui, M.; Nakajima, A. *Chem. Lett.* **2006**, *35*, 888.
- (34) Mitsui, M.; Ando, N.; Nakajima, A. Unpublished Data.
- (35) Rusyniak, M. J.; Ibrahim, Y. M.; Wright, D. L.; Khanna, S. V.; El-Shall, M. S. *J. Am. Chem. Soc.* **2003**, *125*, 12001.
- (36) Alexander, M. L.; Johnson, M. A.; Levinger, N. E.; Lineberger, W. C. *Phys. Rev. Lett.* **1986**, *57*, 976.
- (37) Mitsui, M.; Ando, N.; Kokubo, S.; Nakajima, A.; Kaya, K. *Phys. Rev. Lett.* **2003**, *91*, 153002.
- (38) Matsunuma, S.; Yamaguchi, S.; Hirose, C.; Maeda, S. *J. Phys. Chem.* **1988**, *92*, 1777.
- (39) Arnold, S. T.; Hendricks, J. H.; Bowen, K. H. *J. Chem. Phys.* **1995**, *102*, 39.
- (40) Becker, I.; Cheshnovsky, O. *J. Chem. Phys.* **1999**, *110*, 6288.
- (41) de Boer, R. W. I.; Gershenson, M. E.; Morpurgo, A. F.; Podzorov, V. *Phys. Status Solidi* **2004**, *201*, 1302.
- (42) Piuze, F.; Dimicoli, I.; Mons, M.; Millié, P.; Brenner, V.; Zhao, Q.; Soep, B.; Tramer, A. *Chem. Phys.* **2002**, *275*, 123.
- (43) Eisenstein, I.; Munn, R. W. *Chem. Phys.* **1983**, *77*, 47.
- (44) Sato, N.; Inokuchi, H.; Silinsh, E. A. *Chem. Phys.* **1987**, *115*, 269.
- (45) Hino, S.; Seki, K.; Inokuchi, H. *Chem. Phys. Lett.* **1975**, *36*, 335.

JP801159N